

Heterobifunctional Photoaffinity Probes for Cytochrome P450 2B

Leposava Antonovič,* Petr Hodek,*¹ Stanislav Smrček,† Petr Novák,* Mirek Šulc,*
and Henry W. Strobel‡

*Department of Biochemistry and †Department of Organic Chemistry, Charles University, Hlavova 2030, CZ-128 40, Praha 2, Czech Republic; and ‡Department of Biochemistry and Molecular Biology, The University of Texas Medical School at Houston, P. O. Box 20708, Houston, Texas 77225

Received April 22, 1999, and in revised form July 19, 1999

Three heterobifunctional photoaffinity probes, *N*-(*p*-azidobenzyl)-*N*-methyl-*p*-aminobenzylamine (I), *N*-(*p*-azidobenzyl)-*N*-methyl-*p*-aminophenethylamine (II), and *N*-(*p*-azidophenethyl)-*N*-methyl-*p*-aminophenethylamine (III), were synthesized and characterized. These probes, containing a photolabile azido-group and an amino-group on opposite sides of the molecule, were designed for photoaffinity labeling of the cytochrome P450 (CYP) 2B active site cavity differing in distance from the heme iron. Spectroscopic studies proved that probes I and II coordinated with the heme iron via their amino-group in the enzyme active center, whereas probe III did not. This result in conjunction with data from kinetic studies suggests probes I and II are appropriate for photoaffinity labeling of the CYP 2B active center. Thus, probe II was used to identify amino acid residues within a distance of the probe length (about 16.5 Å) from the heme. Analysis of a Lys-C digest of the probe II-labeled CYP 2B4 revealed a single labeled hexapeptide corresponding to position 192–197 of the CYP 2B4 sequence. Using post-source decay/matrix-assisted laser desorption ionization–time of flight, Arg197 was identified as a probe II target. The location of the labeled site in three-dimensional structures of bacterial CYPs and in CYP 2B homology models is discussed. © 1999 Academic Press

Key Words: cytochrome P450 2B; photoaffinity probe; ligand binding; MALDI-TOF; structure.

Cytochrome P450 (EC 1.14.14.1), a key enzyme of the mixed-function oxidase system, is responsible for

¹To whom correspondence should be addressed. Fax: 420-2-21952331. E-mail: hodek@prfdec.natur.cuni.cz.

the biotransformation of many drugs, environmental pollutants, steroids, fatty acids, and bile acids and frequently for activation of carcinogens (1). That is why the relationship of cytochrome P450 structure to function is of a great importance and has been extensively studied. However, our full understanding of this relationship has been limited by the lack of three-dimensional (3D)² structures for mammalian isoenzymes. Mammalian isoforms of CYPs are integral membrane proteins of either mitochondria or the endoplasmic reticulum, in contrast to those isolated from bacteria, which are soluble cytosolic enzymes. To date, five bacterial CYP tertiary structures were determined using X-ray crystallography (2–6): CYP 101 (P450cam), CYP 108 (P450terp), CYP 102 (P450BM-3), CYP 107A1 (P450eryF), and CYP 55A1 (P450nor). As there are significant similarities among the structures of bacterial CYPs, the presumption of a “structural core” common to all CYPs has been made. Thus, 3D models of mammalian CYPs based on expected global structure homology with bacterial CYPs have been constructed (7, 8). However, CYP 101 of *Pseudomonas putida* shares only 10–20% sequence identity with the mammalian CYPs. The validity of using bacterial CYPs as templates for mammalian 3D models has not yet been clearly established, although most structural studies on mammalian CYPs based predominantly on a CYP

² Abbreviations used: CYP, cytochrome P450; PB, phenobarbital; Ms, liver microsomes; 3D, three dimensional; PSD, postsource decay; *K*_s, spectral dissociation constant; ΔA_{\max} , absorption difference at saturation; GSH, reduced glutathione; DIA, diamantane; PR, 7-pentoxerysoruflin; PDB, protein data bank; MALDI-TOF, matrix-assisted laser desorption ionization–time of flight; MS, mass spectra; EI, electron impact; TFA, trifluoroacetic acid; BCA, bicinchonic acid; [M+H]⁺, protonated molecular mass; Lys-C, endoproteinase cleaving peptide bonds C-terminally at lysine.

102 template have been supportive of the structure-sequence analogue.

Beside 3D homology models, a number of other techniques have been used to locate enzyme active sites, including spectroscopic techniques, site-directed mutagenesis studies, and protein modification approaches using mechanism-based inhibitors and affinity or photoaffinity probes to determine critical amino acids involved in substrate binding.

Photoaffinity labeling usually requires chemical derivatization of the substrate with a photolabile group. An irradiation of a binary complex (protein-photolabile substrate) causes the formation of a reactive intermediate that binds covalently to the enzyme (9). This technique was successfully applied for labeling of several CYPs, revealing some active center amino acids (10, 11).

Benzphetamine is an amphetamine with pronounced sympathomimetic stimulant activity in the central nervous system (12). This compound has high turnover numbers with several CYPs. As the highest affinity was determined for CYP 2B1 ($K_m = 1.8 \times 10^{-4}$ M and $K_s = 5.5 \times 10^{-5}$ M) (13), benzphetamine is frequently used as a specific substrate for CYP 2B1. It was shown earlier that desmethylbenzphetamine was also N-demethylated in the same manner as benzphetamine and its affinity for CYP was comparable to that of benzphetamine. Derivatives of desmethylbenzphetamine were successfully used as photoaffinity probes. The introduction of photolabile azido groups into a desmethylbenzphetamine skeleton did not cause any significant changes of the CYP binding affinity, compared to benzphetamine (10, 14).

In this paper we report a study of CYP 2B interactions with heterobifunctional photoaffinity probes (varying in their lengths) derived from benzphetamine structure. The probes contain azido- and amino-groups on the opposite ends of their molecules. The aim of the amino-group is to anchor the probe to the heme while the azido group is able (after photoactivation) to bind accessible amino acids in the active center cavity of CYP. Use of a probe matching the molecular size of benzphetamine for photoaffinity labeling of CYP 2B4 resulted in a covalent modification of Arg197.

EXPERIMENTAL PROCEDURES

Materials. Coomassie brilliant blue R250 and 7-pentoxoresorufin were products of Fluka (Germany). Phenobarbital was purchased from Kulich (Czech Republic). Reduced glutathione (GSH) and silica gel TLC plates were obtained from Merck (Germany). NADPH was purchased from Reanal (Hungary), and TFA and somatostatin were from Aldrich (Czech Republic). Bicinchonnic acid (BCA) was obtained from Sigma (U.S.A.). Diamantane was a gift from Ing. Janku (Prague Institute of Chemical Technology, Czech Republic). Endoproteinase Lys-C (from *Lysobacter enzymogenes*) was a product of Promega. All other chemicals were of analytical grade or better.

Synthesis of photoaffinity probes. Aminoazido probes, *N*-(*p*-azidobenzyl)-*N*-methyl-*p*-aminobenzylamine · HCl (I), *N*-(*p*-azidobenzyl)-*N*-methyl-*p*-aminophenethylamine · HCl (II), and *N*-(*p*-azidophenethyl)-*N*-methyl-*p*-aminophenethylamine · HCl (III), were prepared by partial reduction of diazido-compounds, *N*-(*p*-azidobenzyl)-*N*-methyl-*p*-azidobenzylamine · HCl (IV), *N*-(*p*-azidobenzyl)-*N*-methyl-*p*-azidophenethylamine · HCl (V), and *N*-(*p*-azidophenethyl)-*N*-methyl-*p*-azidophenethylamine · HCl (VI), which were synthesized according to Hodek and Strobel (14).

In brief, the diazidoderivative (0.3 mmol) was dissolved in 20 ml ethyl alcohol and 50 mg of potassium carbonate was added to the solution. Then, a solution of 24 mg (0.15 mmol) of DL-dithiothreitol in 2 ml ethyl alcohol was added with stirring. The reaction mixture was stirred at room temperature for 4 h. The conversion of the azido-groups to amino-groups was monitored by HPLC at 254 nm (Sepharon SGX column, 3.3×150 mm, Tessek, Czech Republic; mobile phase, 10% methanol in diethyl ether) to obtain the maximal amount of corresponding aminoazide in comparison to the original diazide and the diamine formed simultaneously. Under optimized conditions at the end of the reduction the reaction mixture consisted of diazide (46%), diamine (13%), and aminoazides (41%) in preparation of probe II. The resulting product was isolated and purified using preparative TLC (silica gel plates, dichloromethane/ethyl acetate, 60/40) and converted to its hydrochloride. The final yields of probes I, II, and III were 16, 35, and 13%, respectively.

The synthesized probes were identified by MS (INCOS 50, Finnigan MAT), IR (PE 684), and NMR (Varian UNITY-INOVA 400). Probe I—MS spectrum (base); EI [m/z (relative intensity %)] 267(M^+ , 8), 133(5), 106(100), 77(62), 51(36), 42(11); IR (CHCl_3) 2098 cm^{-1} (N_3); $^1\text{H NMR}$ (CD_3OD) 7.98(d; $J = 8.5$; 2H); 7.81(d; $J = 8.5$; 2H); 7.74(d; $J = 8.5$; 2H); 7.37(d; $J = 8.5$; 2H), /all Ar-H/; 4.74(m; 2H), /N- CH_2 /; 4.55(m; 2H), /N- CH_2 /; 2.91(s; 3H), /N- CH_3 /. Probe II—MS spectrum (base); EI 281(M^+ , 3), 175(69), 147(3), 132(46), 120(12), 104(100), 86(21), 77(57), 42(57); $^1\text{H NMR}$ (CDCl_3) 7.27(d; $J = 8.5$; 2H); 6.62(d; $J = 8.5$; 2H); 6.96 (d; $J = 8.5$; 4H), /all Ar-H/; 3.51(s, 2H), /N- CH_2 /; 2.70(m, 2H); 2.58(m, 2H), / CH_2 - CH_2 /; 2.25(s, 3H), /N- CH_3 /. Probe III—MS spectrum (base), EI 295(M^+ , 0.1), 267(8), 196(3), 145(2), 133(3), 118(2), 106(100), 77(22), 51(10), 42(14); IR (CHCl_3), N_3 band present; $^1\text{H NMR}$ (CD_3OD) 7.78(d; $J = 8.4$; 2H); 7.69(d; $J = 8.4$; 2H); 7.57(d; $J = 8.4$; 2H); 7.24(d; $J = 8.4$; 2H), /all Ar-H/; 3.5-3.7(m, 4H); 3.3-3.5(m, 4H), / CH_2 - CH_2 /; 3.23(s, 3H), /N- CH_3 /. Probe IV—MS spectrum (base); EI 293(M^+ , 7), 194(2), 145(3), 132(8), 104(100), 77(49), 42(32); IR (CHCl_3) 2117 cm^{-1} (N_3). Probe V—MS spectrum (base) EI 307(M^+ , only detected), 279(2), 175(56), 149(10), 132(33), 104(100), 77(81), 51(29), 42(33); IR (CHCl_3), N_3 band present; $^1\text{H NMR}$ (CDCl_3) 7.25(d; $J = 9.6$; 2H); 7.15(d; $J = 8.4$; 2H); 6.91-7.00(m, 4H), /all Ar-H/; 3.51(s; 2H), /N- CH_2 -arom./; 2.78(t; $J = 7.8$; 2H), 2.60(t; $J = 7.8$; 2H), / CH_2 - CH_2 /; 2.26(s; 3H)/ CH_3 /. Probe VI—MS spectrum (base) EI 293(14), 267(2), 149(5), 132(9), 118(2), 104(100), 77(75), 51(31), 42(33); IR (CHCl_3), 2117 cm^{-1} (N_3); $^1\text{H NMR}$ (CD_3OD) 7.54(d; $J = 8.2$; 4H); 7.24(d; $J = 8.2$; 4H), /all Ar-H/; 3.6(m, 4H); 3.3(m; 4H), / CH_2 - CH_2 /; 3.21(s; 3H), /N- CH_3 /. Molar absorption coefficients of probes I, II, III, IV, V, and VI (in methanol solutions) were determined spectrophotometrically at 254 nm (azido-group absorption maximum) to be 2.44, 2.64, 2.36, 2.85, 3.41, and 2.82×10^4 $\text{mol}^{-1} \times \text{liter}$, respectively.

Isolation of microsomal fractions and pure isoenzyme. Liver microsomal fractions (Ms) of phenobarbital (PB)-treated rats or rabbits were prepared according to Guengerich (15). CYP 2B4 was isolated from rabbit PB Ms as described by Haugen and Coon (16).

Cytochrome P450 difference spectra. Cytochrome P450 difference spectra with photoaffinity probes were recorded on a Specord M-40 spectrophotometer (Carl Zeiss, Jena, Germany). Rat PB Ms and pure isoenzyme CYP 2B4 were diluted with phosphate buffer (0.1 M K/PO_4 , pH 7.4, with 20% glycerol) to 3.3 nmol P450/ml and 2 nmol P450/ml, respectively. After recording the baseline, the contents of the sample cuvette was treated with a gradually increasing amount

of photoaffinity probe tested (final conc, 2–700 μM), and the same volume of the probe solvent (water) was added to the reference cuvette. The difference spectra were thereby recorded from 350 to 500 nm.

Inhibition studies. The inhibitory effects of the probes on dephenylase activity in PB-induced microsomes were determined using a Perkin–Elmer LS-5B spectrofluorimeter (17). A microsomal solution was diluted with the phosphate buffer (0.1 M K_2PO_4 , pH 7.2 with 20% glycerol) to the final concentration of 0.05 nmol P450/ml and placed into the fluorimeter cuvette. For each 7-pentoxoresorufin concentration (0.5, 1.0, 2.5, and 5.0 μM) the inhibitory effects of photoaffinity probes in various concentrations (5, 10, 20, and 50 μM) was tested by recording the time course of relative fluorescence increase (within 10 min), corresponding to resorufin production.

Probe half-life determination. All photolyses were carried out in quartz cuvettes (1-cm pathlength, 3 ml) at room temperature using a photolyzer purchased from Oriol Corp. (Stratford, CT) equipped with a 100-W mercury Arc lamp as described by Hodek and Strobel (14).

To determine half-lives of probes upon irradiation, their methanol solutions (0.05 mM) were photolyzed for 0, 1, 4, 8, and 16 s, followed by recording their spectra between 200 and 450 nm. The half-lives were estimated from linearized decay curves plotted for each of the compounds based on the disappearance of their azido-group absorption maxima at ~ 254 nm.

Preparative photolabeling of CYP 2B4. Photoaffinity labeling of CYP 2B4 was carried out in quartz tubes (i.d. 4 mm) at room temperature using the photolyzer described above.

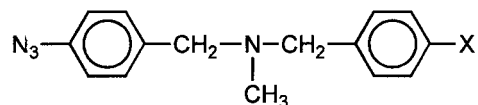
Samples of CYP 2B4 diluted with Tris–HCl (10 mM, pH 7.2) to the final concentration of 4 nmol P450/ml containing 25 μM probe II were photolyzed for 20 s in the presence or absence of 6 μM diamantane (DIA). Immediately after the photolysis glutathione was added to the final concentration of 12.5 $\mu\text{mol/ml}$. As a control sample, the irradiated reaction mixture, consisting of a pure enzyme, solvent for the photoaffinity probe (water), and DIA (methanol), was used. Then, the samples were diluted 1:1 (v/v) with electrophoresis sample reducing buffer and subjected to electrophoresis (10% separating gel) (18) in order to remove minor protein impurities and photodegradation products prior to the analysis of photoaffinity-labeled CYP 2B4 on MALDI-TOF.

Analysis of labeled CYP 2B4. The protein band, corresponding to CYP 2B4, was excised from the gel and digested by Lys-C directly in the gel as described by Shevchenko *et al.* (19). Resulting peptide mixtures were subjected to MALDI-TOF mass spectrometer Bruker BIFLEX (Bruker-Franzen) equipped with a nitrogen laser (337 nm) and a delayed extraction ion source. Positive-ion mass spectra of peptide maps were measured in the reflection mode. A saturated solution of α -cyano-4-hydroxycinnamic acid in aqueous 30% acetonitrile and 0.1% TFA was used as a MALDI matrix. One microliter of the sample and 1 μl of the matrix solution were mixed on the target and allowed to dry at the ambient temperature. Spectra were internally calibrated by employing the monoisotopic $(\text{M}+\text{H})^+$ ion of peptide standard (somatostatin). Postsorce decay (PSD) spectra were recorded in 12 segments, with each succeeding segment representing a 30% reduction in reflector voltage. Segments were pasted, calibrated, and smoothed under computer control by Bruker XTOF 3.0 software.

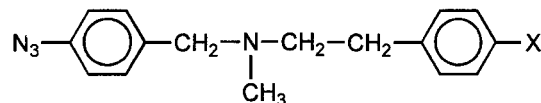
Analytical methods. Protein concentration in the microsomal fractions was determined by the BCA method (20). The concentration of cytochrome P-450 was estimated according to method by Omura and Sato (21) based on the complex of reduced P-450 with CO.

RESULTS

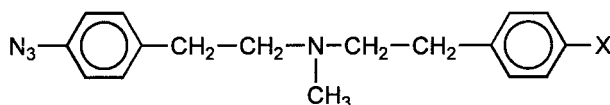
Three aminoazido photoaffinity probes were synthesized by partial reduction of corresponding diazido derivatives (Fig. 1). Chemical structures of all the com-



X = NH_2 - N-(p-azidobenzyl)-N-methyl-p-aminobenzylamine (I)
X = N_3 - N-(p-azidobenzyl)-N-methyl-p-azidobenzylamine (IV)



X = NH_2 - N-(p-azidobenzyl)-N-methyl-p-aminophenethylamine (II)
X = N_3 - N-(p-azidobenzyl)-N-methyl-p-azidophenethylamine (V)



X = NH_2 - N-(p-azidophenethyl)-N-methyl-p-aminophenethylamine (III)
X = N_3 - N-(p-azidophenethyl)-N-methyl-p-azidophenethylamine (VI)

FIG. 1. Structures of homo- and heterobifunctional photoaffinity probes.

pounds were confirmed by NMR and mass spectroscopy. The probe photolability was measured as a time course of disappearance of their azido-group absorption maxima upon irradiation with UV light. Aminoazido probes (I–III) showed half-lives around 3 s while their diazido analogues (IV–VI) were more photolabile having half-lives of about 2 s.

The interaction of the probes (aminoazido and diazido) with CYP of PB-induced liver microsomes and purified 2B4 were examined by difference spectroscopy. From the difference spectra of PB-induced Ms with each photoaffinity probe, spectral dissociation constants were determined to be within the range of 1–40 μM . According to the position of spectral maxima and minima the probes were classified as compounds coordinating heme iron, heme ligands, (maximum ~ 432 nm and broad minimum ~ 415 nm) or compounds not coordinating the heme iron (maximum ~ 387 nm and minimum ~ 418 nm).

Based on the results obtained from the difference spectra of PB Ms as well as the pure CYP 2B4 with photoaffinity probes, only probes I and II were found to bind the CYP as heme ligands. Hence, these compounds were selected as potential photoaffinity probes for mapping of the CYP active center within the differing distances from the heme. Probe II, having the structure most similar to that of the parent molecule, benzphetamine, was examined in this paper.

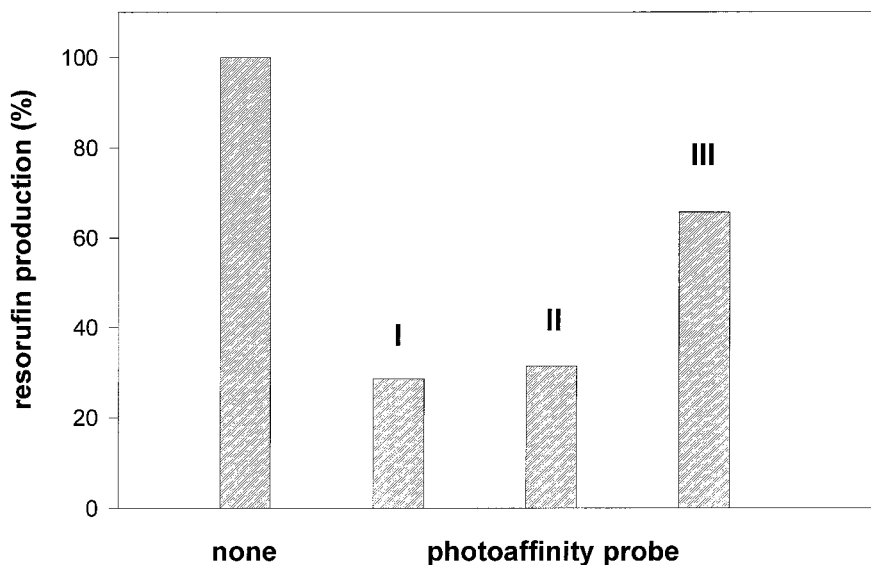


FIG. 2. Inhibition effect of photoaffinity probes on 7-pentoxoresorufin O-dealkylation in PB Ms. The probes were used in 10 times molar excess to substrate.

To examine further the interactions of the amino-group containing probes I–III with CYP 2B4, the inhibition of 7-pentoxoresorufin (PR) O-dealkylation was tested in PB Ms using a 10 times molar excess of probe to substrate (see Fig. 2). Photoaffinity probe III, which previously showed no heme coordination in difference spectra, also exerted the weakest inhibitory capability, in comparison to the other probes. Thus, more detailed inhibition studies were performed with probes I and II, which revealed $K_i = 5\text{--}10 \mu\text{M}$ and $K_i = 7\text{--}14 \mu\text{M}$, respectively.

Probe II was employed for photoaffinity labeling of purified CYP 2B4. In addition to labeling CYP 2B4 with the probe, CYP 2B4 labeling was also performed in the presence of the probe II competitor, DIA. The role of DIA was to prevent probe incorporation into the enzyme active center and thus to assess the specificity of probe labeling. Samples of photoaffinity labeled CYP 2B4 were then digested by proteinase Lys-C and the mixture of resulting CYP 2B4 peptides was analyzed on a MALDI-TOF apparatus. Using this technique, masses of the individual peptides were determined in each sample (see Fig. 3). From the comparison of MALDI-TOF-MS spectra in Figs. 3a–3c it is clear that the peak having the mass of 997.6 (marked by asterisk) occurs only in the sample irradiated in the absence of DIA. In other words, this peak corresponds to the peptide–probe adduct originating from the enzyme active center. The labeled peptide exactly matched the theoretic molecular weight of hexapeptide DPVFLR from positions 192–197 of a CYP 2B4 primary structure (see Table I). Table I summarizes the peptide masses of all three CYP 2B4 sample digests determined by MALDI-TOF and the masses calculated based on presumed

peptide compositions as well as positions of these peptides in the CYP 2B4 sequence. To prove the deduced hexapeptide sequence and identify the covalently modified amino acid, PSD/MALDI-MS analysis of the adduct was performed. Data shown in Fig. 4 confirm the expected amino acid sequence of the labeled peptide and indicate Arg197 to be involved in the adduct formation. This result demonstrates that photoaffinity probe II is well suited for photoaffinity labeling of CYP 2B4.

DISCUSSION

The photoaffinity probes (I, II, and III) as well as the previously reported diazido-probe are based on the structure of benzphetamine, a compound having a high binding affinity for the active center of CYP 2B (10). In contrast to diazido-probes used for crosslinking within the enzyme active center, the newly synthesized aminoazido-derivatives are designed to label the CYP 2B binding site and/or access channel with differing distances from the heme. These derivatives are expected to be linked to the heme iron as its sixth ligand via their amino-group, while the opposite end of the molecule (containing the photolabile azido-group) is located in distal regions of the active center cavity. A similar approach using the heme binding compound 1-(4-azidophenyl)imidazole was applied by Swanson and Dus (22) for photoaffinity labeling of CYP 101.

To determine whether the photoaffinity probes bind the heme iron as its ligands, difference spectroscopy was employed, since this technique allows the direct examination of changes in heme iron coordination (17). As controls, diazido-analogues of all probes (missing a

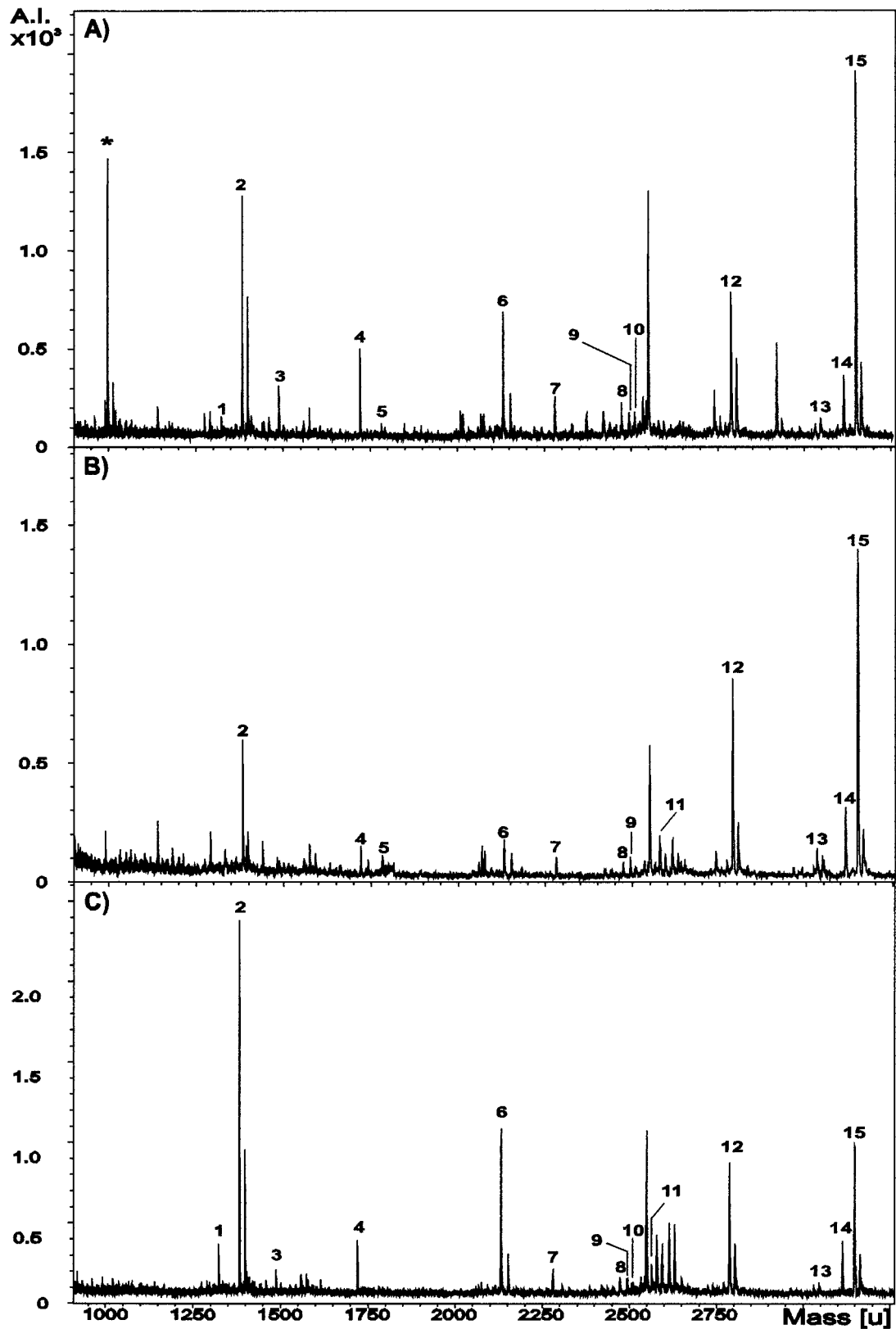


FIG. 3. MALDI-MS spectrum of a Lys-C peptide mixture of CYP 2B4, labeled with probe II in the absence of diamantane (a), labeled with probe II in the presence of diamantane (b), or photolyzed without probe II (c). Labeled peptide is marked by an asterisk.

TABLE I
Experimental (MALDI-MS) and Calculated Data
for CYP 2B4 Lys-C Peptides

Peak No.	Measured mass [M+H] ⁺			Calculated mass [M+H] ⁺	Sequence position
	A	B	C		
*	997.59	n.d.	n.d.	997.55	192–197
1	1323.70	n.d.	1323.74	1323.70	374–384
2	1382.76	1382.68	1382.68	1382.68	422–433
3	1487.87	n.d.	1487.94	1487.91	50–61
4	1719.94	1719.85	1719.88	1719.88	237–251
5	1781.95	1781.92	n.d.	1781.91	385–400
6	2131.18	2131.02	2131.08	2131.12	327–345
7	2280.28	2280.24	2280.11	2280.19	233–251
8	2472.42	2472.30	2472.32	2472.29	140–159
9	2493.40	2493.22	2493.28	2493.28	254–274
10	2509.32	n.d.	2509.27	2509.22	401–422
11	n.d.	n.d.	2563.43	2563.42	26–49
12	2786.55	2786.44	2786.55	2786.43	252–274
13	3047.64	3047.46	3047.42	3047.66	160–187
14	3112.64	3112.59	3112.50	3112.60	226–251
15	3147.65	3147.65	3147.57	3147.67	346–373

Note. n.d., not detectable. Labeled peptide (adduct) is marked by an asterisk. Peak numbering refers to Fig. 3. CYP 2B4 was photolyzed in the presence of probe II (A), in the presence of probe II and diamantane (B), or in the absence of these compounds (C).

primary amino-group) were used. The difference spectra of CYP 2B4 with probes I and II revealed a pronounced shift of an absorption maximum to about 432 nm (Type II binding spectra), indicating the changes of heme coordination by primary amines. Since this type of binding spectra was not detectable with diazido-probes (IV–VI), it indicates that the amino-groups of probes I and II are responsible for their heme binding. On the other hand, probe III was oriented in the active center in a different way since only Type I binding spectra were detected. Presumably, the amino-group of probe III (the longest probe) is located in more polar regions of the active center cavity having too long a distance from the heme to allow the same kind of iron atom coordination. In addition, 7-PR dealkylase activity was inhibited more strongly by probes I and II in comparison with probe III, suggesting their potential interaction with iron. Thus, the heme-binding probes (I and II), showing a strong binding to the enzyme active center, are suggested to be well suited for photoaffinity labeling of CYP 2B. In this paper, we deal with photoaffinity labeling of CYP 2B4 by medium-length probe II, which more nearly matches the molecular size of benzphetamine.

Upon UV irradiation a side group of the probe is photolyzed to a nitrogen molecule and a nitrene intermediate. This reactive intermediate is known to react preferentially with electron-rich groups of polar amino acids, e.g., Lys and Arg (9), or undergo rearrangements

resulting in long-lived derivatives. To reduce non-specific labeling caused by these rearrangement products we successfully used GSH as a quencher. Using the reaction conditions optimized earlier (10) with respect to the probe/CYP 2B4 molar ratio, duration of photolysis, and scavenger addition, highly specific labeling of the target CYP 2B4 enzyme was achieved. MALDI-TOF analysis of a Lys-C digest of labeled CYP 2B4 revealed a single peak, whose mass exactly matched a potential peptide–probe adduct (see Table I). Moreover, this peak was not detectable in a control sample of CYP irradiated in the absence of the probe. To confirm that the labeled peptide originates from the enzyme active center, additional photoaffinity labeling experiments were carried out in the presence of a specific CYP 2B4 substrate, diamantane (23), that is able to displace another compound from the active center (24). This bulky hydrocarbon, of a high binding affinity for CYP 2B, completely prevented probe incorporation. Thus, the peak of a potential peptide–probe adduct was not detectable under these conditions. Hence, we conclude that identified peptide DPVFLR (192–197) is located in the enzyme substrate binding site and/or an access channel.

The PSD/MALDI-MS analysis of the adduct confirmed the expected amino acid composition and localized the position of the probe incorporation at Arg197 residue. In accordance with the known labeling specificity of nitrene intermediates the probe modified an electron-rich amino acid residue in its vicinity.

The principal objective of this study is to identify active site amino acid residues of CYP 2B4. Probe II, owing to its amino-group, is, upon binding to CYP 2B4, anchored to the heme iron and the probe-photogenerated nitrene is able to label regions of the active center and/or the substrate access channel at a specific distance from the heme. Taking into account the length of the extended probe (about 14.5 Å) (10) and a distance between the heme iron atom and the nitrogen atom of the probe amino-group (about 2 Å) (25), the target of probe II labeling, Arg 197, should be located within the distance of 16.5 Å from the heme. In addition to other techniques revealing the structural significance of numerous amino acids of microsomal CYPs (e.g., substrate docking and site-directed mutagenesis experiments), our finding on the location of a particular amino acid residue, Arg 197, will contribute to the process of optimizing and/or evaluating 3D homology models of CYP 2B.

Since crystal structures of bacterial CYPs are frequently used as templates for 3D homology models of microsomal CYPs, we attempted to assign the labeled peptide to the molecular topology of bacterial CYPs. Because of a rather low sequence homology (about 20%) between CYP 2B4 and bacterial CYPs, the position of the labeled peptides was located using a com-

On the other hand, the most recent paper on 3D models of CYP 2 family (8), built on the basis of CYP 102 template, unfortunately, does not deal in detail with a model of CYP 2B. Furthermore, due to a different alignment strategy used, the labeled residue lies far from the putative access channel. The labeled peptide 192–197 is assigned to a segment connecting helices D1 and E. Although the models discussed were optimized to fit data of site-directed mutagenesis studies and CYP 2B4 substrate docking, their validity should be confirmed by also employing data from photoaffinity labeling experiments. From this point of view it would be of great interest to examine the 3D models by docking of the photoaffinity probe II.

In conclusion, the heme binding photoaffinity probe of benzphetamine size, presented here, was used to identify amino acid residue Arg 197, which is most likely involved in the upper part of the active center or a substrate access channel structure of CYP 2B4.

ACKNOWLEDGMENT

This study was supported by Grant VS 96141 from The Czech Ministry of Education.

REFERENCES

- Porter, T. D., and Coon, M. J. (1991) *J. Biol. Chem.* **266**, 13469–13472.
- Poulos, T. L., Finzel, B. C., Gunsalus, I. C., Wagner, G. C., and Kraut, J. (1985) *J. Biol. Chem.* **260**, 16122–16130.
- Hasemann, C. A., Ravichandran, K. G., Peterson, J. A., and Deisenhofer, J. (1994) *J. Mol. Biol.* **236**, 1169–1185.
- Ravichandran, K. G., Bodupalli, S. S., Hasemann, C. A., Peterson, J. A., and Deisenhofer, J. (1993) *Science* **260**, 731–736.
- Cupp-Vickery, J. R., and Poulos, T. L. (1995) *Struct. Biol.* **2**, 144–153.
- Park, S. Y., Shimizu, H., Adachi, S., Nakagawa, A., Tanaka, I., Nakahara, K., Shoun, H., Obayashi, E., Nakamura, H., Iizuka, T., and Shiro, Y., (1997) *Nat. Struct. Biol.* **4**, 827–832.
- Chang, Y.-T., Stiffelman, O. B., Vakser, I. A., Loew, G. H., Bridges, A., and Waskell, L. (1997) *Protein Eng.* **10**, 119–129.
- Lewis, D. F. V. (1998) *Xenobiotica* **28**, 617–661.
- Bayley, H. (1983) in *Photogenerated Reagents in Biochemistry* (Work, T. S., and Burdon, R. H., Eds.), 2nd ed., Elsevier Science, Amsterdam.
- Cvrk, T., Hodek, P., and Strobel, H. W. (1996) *Arch. Biochem. Biophys.* **330**, 142–152.
- Cvrk, T., and Strobel, H. W. (1998) *Arch. Biochem. Biophys.* **349**, 95–104.
- Caldwell, J. (1980) *Amphetamines and Related Stimulants: Chemical, Biological, and Sociological Aspects*, CRC Press, Boca Raton.
- Lau, P. P., and Strobel, H. W. (1982) *J. Biol. Chem.* **257**, 5257–5262.
- Hodek, P., and Strobel, H. W. (1994) *Bioorg. Chem.* **22**, 253–267.
- Guengerich, F. P. (1977) *J. Biol. Chem.* **252**, 3970–3979.
- Haugen, D. A., and Coon, M. J. (1976) *J. Biol. Chem.* **251**, 7929–7939.
- Rutten, A. A. J. J. L., Falke, H. E., Catsburg, J. F., Wortelboer, H. M., Blaauboer, B. J., Doorn, L., van Leeuwen, F. X. R., Theelen, R., and Rietjens, I. M. C. M. (1992) *Arch. Toxicol.* **66**, 237–244.
- Laemmli, U. K. (1970) *Nature* **227**, 680–685.
- Shevchenko, A., Wilm, M., Vorm, O., and Mann, M. (1996) *Anal. Chem.* **68**, 850–858.
- Wiechelmann, K. J., Braun, R. D., and Fitzpatrick, J. D. (1988) *Anal. Biochem.* **175**, 231–237.
- Omura, T., and Sato, R. (1964) *J. Biol. Chem.* **239**, 2370–2378.
- Swanson, R. A., and Dus, K. M. (1979) *J. Biol. Chem.* **254**, 7238–7246.
- Hodek, P., Janscak, P., Anzenbacher, P., Burkhard, J., Janku, J., and Vodicka, L. (1988) *Xenobiotica* **18**, 1109–1118.
- Hodek, P., Burkhard, J., and Janku, J. (1995) *Gen. Physiol. Biophys.* **14**, 225–239.
- Poulos, T. L., and Howard, A. J. (1987) *Biochemistry* **26**, 8165–8174.
- Szklarz, G. D., He, Y. A., and Halpert, J. R. (1995) *Biochemistry* **34**, 14312–14322.
- Szklarz, G. D., Ornstein, R. L., and Halpert, J. R. (1994) *J. Biomol. Struct. Dyn.* **12**, 61–78.
- Nelson, D. R., and Strobel, H. W. (1988) *J. Biol. Chem.* **263**, 6038–6050.
- Heinemann, F. S., and Ozols, J. (1983) *J. Biol. Chem.* **258**, 4195–4201.